

# Mobile Cloud Platform for Breast Cancer Diagnosis Using Deep Learning

<sup>\*1</sup>AreejRebat Abed,<sup>\*2</sup> Dr.Karim Q. Hussein

<sup>\*1</sup> Computer Science, Iraqi commission for computer and informatics, Informatics Institute for Postgraduate Studies, Baghdad, Iraq. areejaa372@gmail.com

<sup>\*2</sup> Assist. Prof. /Computer Science Dept./Faculty of Science/ Mustansiriyha University / Baghdad, Iraq . Karimzzm@yahoo.com , karim.q.h@uomustansiriyha.edu.iq

**Abstract:** The development of mobile technology has led to great advances in providing health services in many developed countries. In this research, cloud computing technology (MCC) was used through the use of mobile applications to employ a mobile health system. In this method, the mammogram image is transferred from the x-ray machine to the cloud using the Android platform in client-side. The technique used to detect breast cancer is the use of the convolutional neural network of the X-ray system to classify a mammogram into benign calcification, benign mass, malignant Calcification, malignant Mass, and normal. Because convolutional neural networks (CNNs) accelerate the diagnostic process with the support of a specialist in diagnosing tumors, they are therefore used to test for breast cancer. A set of mammography images were reprocessed to transform a mammogram that is visible to human into an understandable image for the computer. The parameters assigned were appropriate to the CNN classifier, and then trained a set of images as a source of training. Then produced a form to recognition the mammogram image. The results obtained show that the CNN classifier achieved an accuracy reached 91,039 on the DDSM (Digital Database of Screening Mammography) data.

**Keywords:** Deep learning, Convolutional Neural Network, Digital Database of Screening Mammography, Mobile Cloud Computing ,Breast cancer, Mammogram images

## 1. Introduction

The incidence of breast cancer among women has reached 23% of all cancer cases around the world, as it is the main cause of death among women, and the percentage of deaths that occur due to cancer among women is 14% [1] . Every eight to nine women will get breast cancer at some point in their lives in Western countries [2]. In the past few years, instead of using expensive computing resources[3], that can be managed locally, cloud computing has been used. Which can be defined as a service that can be provided upon request through which data can be stored on the network of remote servers for the purpose of managing and processing it. The progress of computer and internet based approach has change the quality of services in healthcare through mobile devices and it use with cloud computing [4]. One of the services provided by cloud computing is a browser-based dashboard that IT personnel can use to access the services provided by the cloud support provider. Updating medical records was easier because cloud computing is suitable for consolidating data stored in the cloud. In addition, there is a large number of resources that can be provided by cloud computing that can hold huge datasets of speech data or medical images[5]. Cloud computing provides many

services that make the healthcare industry provide services without interruption with shorter downtime[6]. There are many patients who suffer from a lack of financial resources, as they can be diagnosed with the help of cloud computing by doctors, also can be provided telehealth[7] and telemedicine[8] to them using cloud computing, which includes move of various medical data, like video recordings and high-resolution medical images of patients from far away areas to Other areas, Where there are doctors .

## 2. Related Work

There is sum of disease diagnostic systems:

- Huang, Qinghua, et al. [9] Introduced a new scheme for computer-assisted diagnostics with human in the ring to help doctors identify breast tumors. The features were acquired via a user-participant role scoring scheme based on BI-RADS lexicon and physician experience.
- Zheng, Jing, et al. [7] combined machine learning methods with methods of feature extraction and selection . The experimental results showed that the high resolution level is 97.2%, the sensitivity is 98.3%, and the specificity is 96.5%, where Adaboost effective breast cancer detection algorithm (DLA-EABA) has been proposed mathematically using advanced computer technologies.
- George, YasmeenMourice, et al. [8] Provide an intelligent system for remote detection and diagnosis of breast cancer patients based on a web service. The cell nuclei locations in the mammograms image were revealed by circular Hough transform and four classification models were used: a multilayer perceptron using a reverse propagation algorithm, a probabilistic neural network (PNN), vector quantization learning, and support vector machine (SVM)
- Aruna, S., L. V. Nandakishore, and S. P. Rajagopalan. [9] proposed for a breast cancer cloud-based decision support system (BCDSS) for diagnosing breast cancer using digital mammography. The system is implemented in a private cloud computing environment and implemented as software / infrastructure as a service to ensure data security and support beginner and expert users.
- Li, Hua, et al. [10] proposed DenseNet Neural Network Model for effective and accurate classification of benign and malignant mammograms. The average resolution of the model is 94.55%

## 3. Proposal System

In this system, a breast cancer diagnostic cloud system was used through which the patient's health data is monitored remotely to diagnose cancer. When analyzing user data that is stored on cloud servers, there will be great flexibility to diagnose and classify different types of diseases. Therefore, here deep convolutional neural network (CNN) developed and is trained to read a set of mammogram images and classify them in the following five cases:

- Normal
- Benign Calcification
- Benign Mass
- Malignant Calcification
- Malignant Mass

Figure 1 shows our proposed architecture[10].An illustration of the proposed structure. In this form, the patient who needs a diagnosis goes to the remote health center in his village, and gives his data to the health service provider, such as x-rays and other health data, where the patient's data is sent to the doctor via the Internet; After that, the doctor uploads the data to the platform of cloud for purpose of processing.

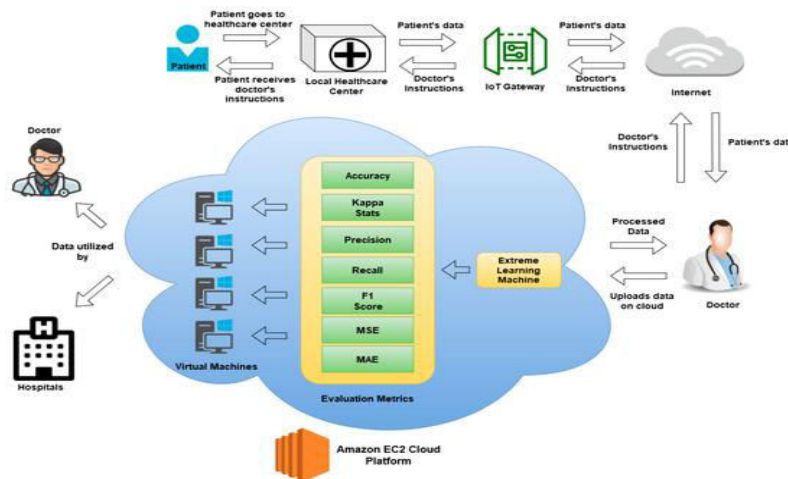


Figure 1: The **proposed** system.

#### 4. Deep Learning

Deep learning algorithms are designed to mimic the function of the human cerebral cortex. These algorithms are representations of deep neural networks, that is, neural networks with many hidden layers [15].

##### 4.1 Convolutional Neural Networks (CNN)

Convolutional neural network (CNN) is one of most widely used in Computer Vision problem, it is a class of Deep Neural Network (DNNs) which based in Multi-Layer Perceptron (MLP) and Back Propagation techniques[11]. It is differing from traditional MLPs by combining a number of locally connected layers that is used for feature extraction, followed by a number of fully connected(FC) layers which is used for classification [12]

#### 5. Data Source

DDSM and CBIS-DDSM databases were used. DDSM (Digital Database for Mammography Screening) is a database of 2,620 mammography status. Contains benign cases, malignant cases, and normal cases with check data of disease. CBIS-DDSM (DDSM Coordinated Breast Imaging Subgroup) is a subset database of the DDSM sponsored by a trained radiographer. DDSM and CBIS-DDSM have two various mammograms - CC (craniofacial - top view) and MLO (lateral oblique - lateral view) that see in Figure 3. The DDSM database contains only normal states. While the abnormal states exist in the CBIS-DDSM sub-database. Generally, 4,091 were used for CNN development

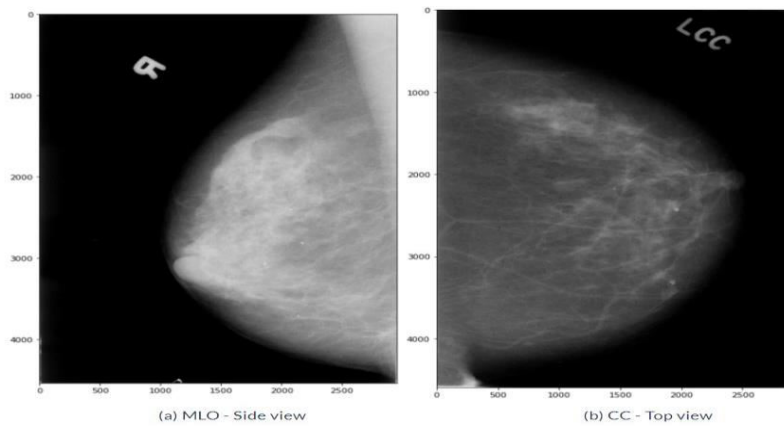


Figure 2. Images of MLO and CC views

## 6. Result and destination: Data Pre-processing

### 6.1 Image Enhancement and Artefacts Removal

Figure 2 shows the original mammography images (see Figure 3-(a)) that contain artefacts that cause a base problem in the CNN development. To eliminate this artefact, a mask has been created for each raw image (Figure 3-(b)) by detecting the largest object in a binary image and filled white gaps (i.e., artefacts) in the background of the image. The region of breast image must separate from the region of a background image using Otsu segmentation method removing artifacts. Then the borders of the mammogram are smoothed with the method of openCvmorphologyEx (see Fig.3 (c)).

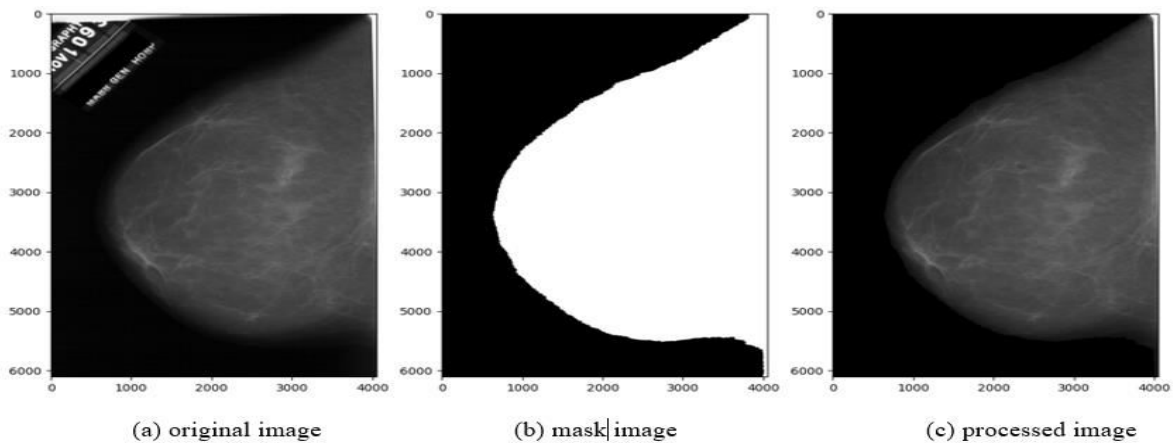


Figure 3. Image Contrast Increase and Artefacts Removal

### 6.2 Patch Extraction

Instead of completely classifying the image, an image correction classifier has been developed, due to the size of the data sets and the available computing power. Therefore, two methods are used to perform correction extraction for abnormal and normal images: In a first way: The natural spots were extracted from inside the image area at random In the second way: spots were created from the abnormal images by gain samples from the centre of the image and around the position of the ROI area.

The figure 4 illustrates the use of the ROI mask image to determine the location and size of the ROI in the abnormal images .

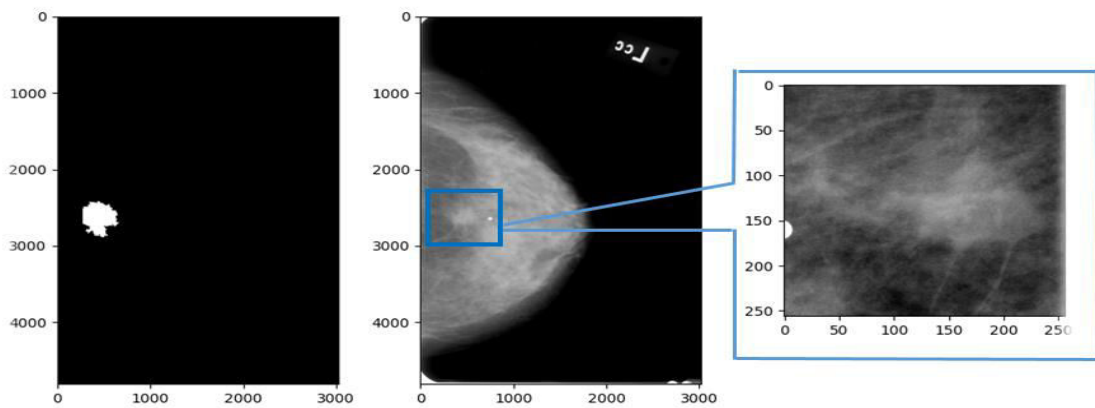


Figure 4. Example of Original, ROI mask, and Patch Images

Generally, was extracted a total of 40,633 patches, 83% of which normal and 17% abnormal (malignant or benign). The purpose of this to show the real-world state. The data that used for training and test purpose is obtained by dividing the extracted corrections into 20% test data and 80% training data. In the test set, 50% of the corrections were isolated to create a validation set. In Figure 5 there are examples of the abnormal stains extracted.

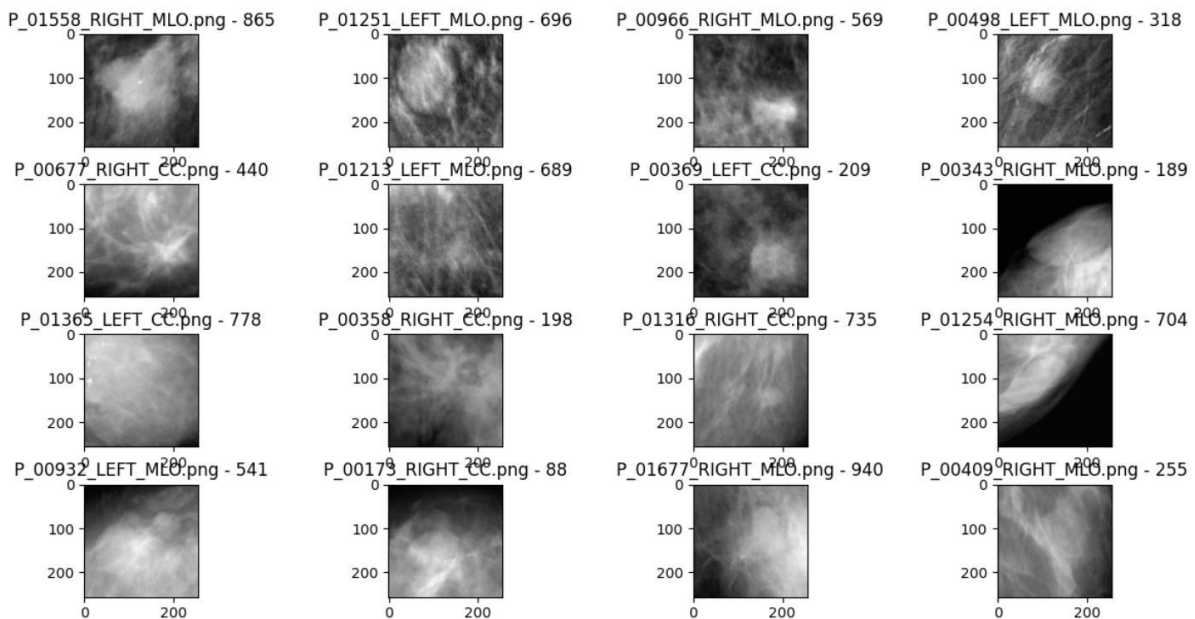


Figure 5. Examples of extracted patch images

### 6.3 Deep CNN Development

#### 6.3.1 Architecture

A basic model is designed with a VGG (Visual Geometry Set) model structure that has a two-layer block wrapping with  $3 \times 3$  micro-filters followed by a maximum aggregation layer. The final model contains four repeating blocks, and each block has a batch leveling layer followed by a maximum aggregate layer and a demolition layer. Each warp layer contains  $3 \times 3$  filters, ReLU activation, and Unified Core Configurator with the same padding to make sure the

output function mappings are the same width and height. The developed CNN architecture is shown in Fig.6-7.

Model: "sequential\_1"

Layer (type)	Output Shape	Param #
conv2d_6 (Conv2D)	(None, 256, 256, 32)	320
batch_normalization_7 (Batch Normalization)	(None, 256, 256, 32)	128
conv2d_7 (Conv2D)	(None, 256, 256, 32)	9248
batch_normalization_8 (Batch Normalization)	(None, 256, 256, 32)	128
max_pooling2d_3 (MaxPooling2D)	(None, 128, 128, 32)	0
dropout_4 (Dropout)	(None, 128, 128, 32)	0
conv2d_8 (Conv2D)	(None, 128, 128, 64)	18496
batch_normalization_9 (Batch Normalization)	(None, 128, 128, 64)	256
conv2d_9 (Conv2D)	(None, 128, 128, 64)	36928
batch_normalization_10 (Batch Normalization)	(None, 128, 128, 64)	256
max_pooling2d_4 (MaxPooling2D)	(None, 64, 64, 64)	0
dropout_5 (Dropout)	(None, 64, 64, 64)	0
conv2d_10 (Conv2D)	(None, 64, 64, 128)	73856
batch_normalization_11 (Batch Normalization)	(None, 64, 64, 128)	512
conv2d_11 (Conv2D)	(None, 64, 64, 128)	147584
batch_normalization_12 (Batch Normalization)	(None, 64, 64, 128)	512
max_pooling2d_5 (MaxPooling2D)	(None, 32, 32, 128)	0
dropout_6 (Dropout)	(None, 32, 32, 128)	0
conv2d_12 (Conv2D)	(None, 32, 32, 256)	295168
batch_normalization_13 (Batch Normalization)	(None, 32, 32, 256)	1024
conv2d_13 (Conv2D)	(None, 32, 32, 256)	590080
batch_normalization_14 (Batch Normalization)	(None, 32, 32, 256)	1024
max_pooling2d_6 (MaxPooling2D)	(None, 16, 16, 256)	0
dropout_7 (Dropout)	(None, 16, 16, 256)	0
flatten_1 (Flatten)	(None, 65536)	0
dense_2 (Dense)	(None, 256)	16777472
batch_normalization_15 (Batch Normalization)	(None, 256)	1024
dropout_8 (Dropout)	(None, 256)	0
dense_3 (Dense)	(None, 5)	1285
Total params: 17,955,301		
Trainable params: 17,952,869		
Non-trainable params: 2,432		

Figure 6 the details of CNN architecture and result output shape each layer.

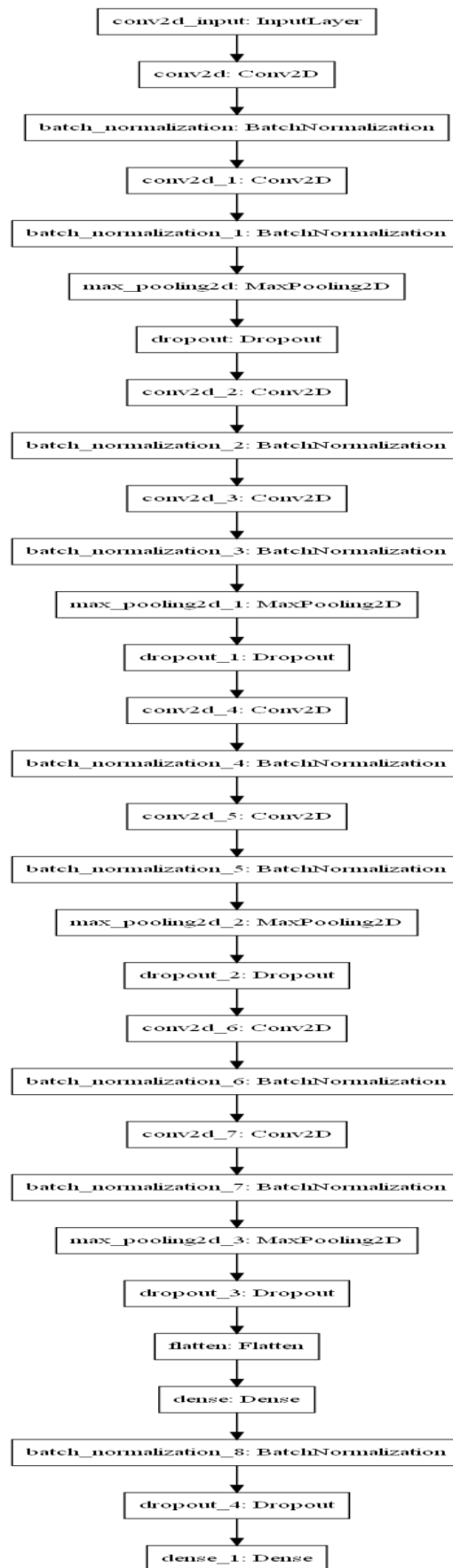


Figure 7. Model architecture

### 6.3.2 Model Improvement and Training Procedure

We see a representation of the accuracy diagram in the training and testing process in Fig. 8. Fig. 9 shows a representation of the loss in this process. A portion of the training and testing result is illustrated in Figure 10. It takes a few hours to complete this process. Here it turns out that when the number of epochs is 25, we will obtain the highest verification accuracy (90.11%) corresponding to the lowest validation loss, so it is considered the optimal number of epochs.

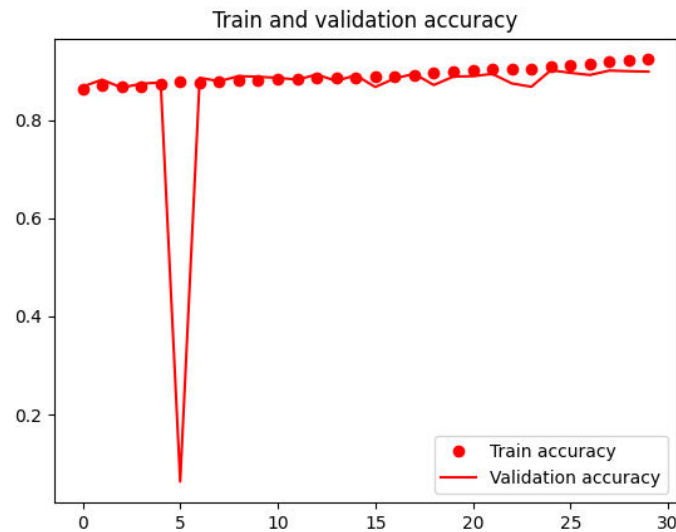


Figure 8: accuracy of Training and validation process

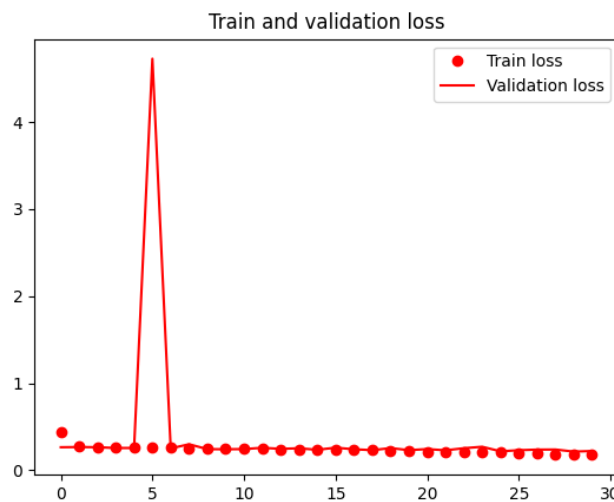


Figure 9: loss of Training and validation process



```

Epoch 21/30
1263/1263 [=====] - 272s 216ms/step - loss: 0.2140 - accuracy: 0.9010 - val_loss: 0.2431 - val_accuracy: 0.8890
Epoch 22/30
1263/1263 [=====] - 272s 215ms/step - loss: 0.2090 - accuracy: 0.9048 - val_loss: 0.2292 - val_accuracy: 0.8937
Epoch 23/30
1263/1263 [=====] - 272s 215ms/step - loss: 0.2090 - accuracy: 0.9043 - val_loss: 0.2532 - val_accuracy: 0.8743
Epoch 24/30
1263/1263 [=====] - 272s 215ms/step - loss: 0.2104 - accuracy: 0.9041 - val_loss: 0.2701 - val_accuracy: 0.8675
Epoch 25/30
1263/1263 [=====] - 273s 216ms/step - loss: 0.2063 - accuracy: 0.9075 - val_loss: 0.2177 - val_accuracy: 0.9011
Epoch 26/30
1263/1263 [=====] - 272s 215ms/step - loss: 0.1970 - accuracy: 0.9121 - val_loss: 0.2302 - val_accuracy: 0.8959
Epoch 27/30
1263/1263 [=====] - 271s 215ms/step - loss: 0.1921 - accuracy: 0.9147 - val_loss: 0.2373 - val_accuracy: 0.8915
Epoch 28/30
1263/1263 [=====] - 271s 215ms/step - loss: 0.1875 - accuracy: 0.9179 - val_loss: 0.2383 - val_accuracy: 0.9005
Epoch 29/30
1263/1263 [=====] - 271s 215ms/step - loss: 0.1813 - accuracy: 0.9207 - val_loss: 0.2143 - val_accuracy: 0.8992
Epoch 30/30
1263/1263 [=====] - 271s 215ms/step - loss: 0.1761 - accuracy: 0.9230 - val_loss: 0.2212 - val_accuracy: 0.8983
> 92.208
> 91.039
142/142 [=====] - 7s 50ms/step - loss: 0.2089 - accuracy: 0.9104
test loss is 0.20888404548168182
test accuracy is 0.9103919267654419
1263/1263 [=====] - 63s 50ms/step - loss: 0.1797 - accuracy: 0.9221
test loss is 0.17974814772605896
test accuracy is 0.9220811128616333

```

Figure 10: Training process and testing process results.

#### 6.4 Computing environment

Typical training in this project was conducted on Windows 10 PC equipped with NVIDIA 16 GB RTX 2080 Super GPU. The CNN model was developed using TensorFlow 2.0 and Keras 2.3.0.

#### 6.5 Examples of Predictions

We can use our ergonomically designed CNN to make predictions about images. Figure (11) and Figure (12) show examples of image projections. The blue color indicates the correct prediction signs, while the red color indicates the wrong prediction addresses. The ratio at the bottom of the image indicates the expected designation.

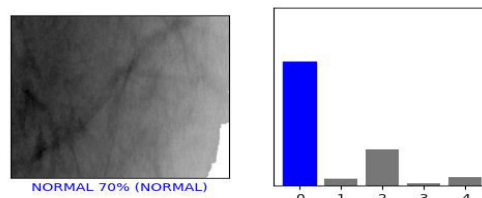


Figure 11. Example of one Image Prediction

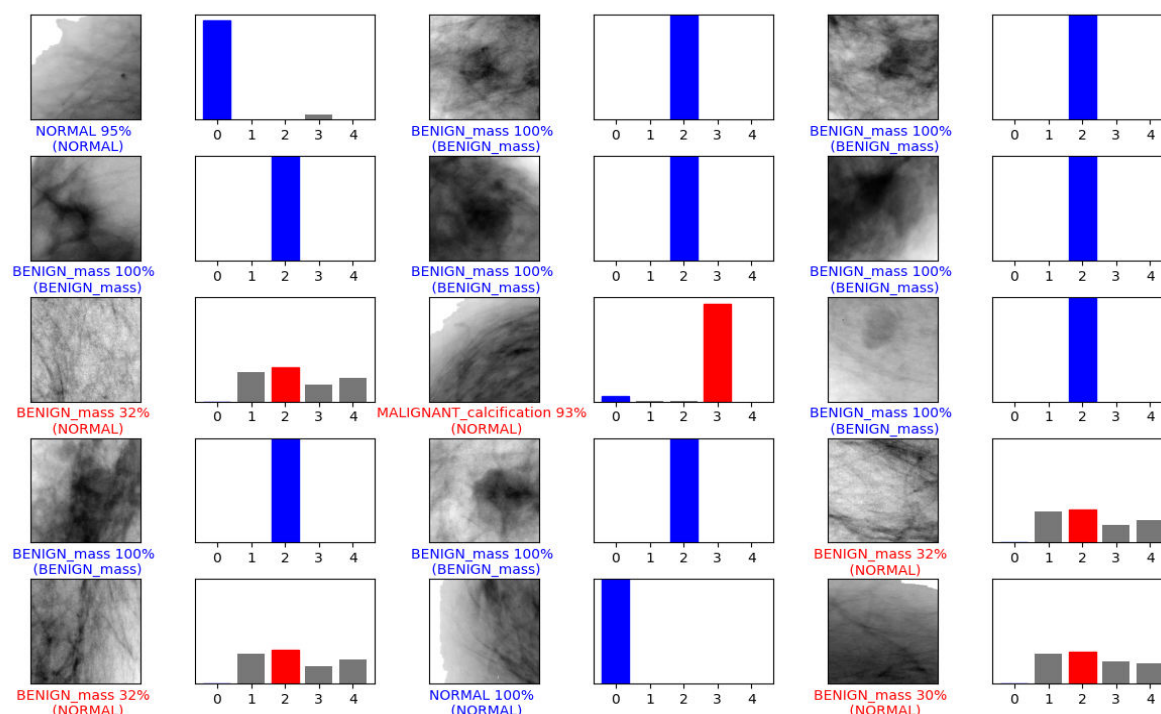


Figure 12. Example of Images Predictions

## 7. Conclusions and Future Studies

In this research, there was propose a cancer prediction approach based on mobile cloud computing. The system combines the cloud high processing power with the massive storage capacity to make it more efficient and convenient. During this project, developed a CNN model for classify mammogram image. Model was trained with greatly imbalanced datasets. The model (i.e., multi-class classification) was trained to classify images in five cases: normal , benign calcification, benign mass , malignant calcification , and malignant mass , with the accuracy of the model, attained at 91.039%, accuracy, however, measurement performance under data conditions Unbalanced is not appropriate.

This project will be expanded by exploring ways to increase the accuracy of the multiple class classification model. An immediate extension of this project is to check model performance after adding additional blocks/layers to the existing CNN model and modifying hyperparameters. Will also improve on the CNN-developed template by integrating it into a complete image classifier.

## 8. References

- S. A. Agnes, J. Anitha, S. I. A. Pandian, and J. D. Peter, "Classification of Mammogram Images Using Multiscale all Convolutional Neural Network (MA-CNN)," *J. Med. Syst.*, 2020, doi: 10.1007/s10916-019-1494-z.
- A. H. Yurttakal, H. Erbay, T. İkizceli, and S. Karaçavuş, "Detection of breast cancer via deep convolution neural networks using MRI images," *Multimed. Tools Appl.*, vol. 79, no. 21–22, pp. 15555–15573, 2020, doi: 10.1007/s11042-019-7479-6.
- A. Al-Fuqaha, M. Guizani, M. Mohammadi, M. Aledhari, and M. Ayyash, "Internet of Things: A Survey on Enabling Technologies, Protocols, and Applications," *IEEE Commun. Surv. Tutorials*, vol. 17, no. 4, pp. 2347–2376, 2015, doi: 10.1109/COMST.2015.2444095.

- T. Saba et al., “Cloud-based decision support system for the detection and classification of malignant cells in breast cancer using breast cytology images,” *Microsc. Res. Tech.*, vol. 82, no. 6, pp. 775–785, 2019, doi: 10.1002/jemt.23222.
- M. A. Mohammed et al., “Voice pathology detection and classification using convolutional neural network model,” *Appl. Sci.*, vol. 10, no. 11, pp. 1–13, 2020, doi: 10.3390/app10113723.
- A. Botta, W. De Donato, V. Persico, and A. Pescapé, “Integration of Cloud computing and Internet of Things: A survey,” *Futur. Gener. Comput. Syst.*, vol. 56, pp. 684–700, 2016, doi: 10.1016/j.future.2015.09.021.
- E. R. Dorsey and E. J. Topol, “State of Telehealth,” *N. Engl. J. Med.*, vol. 375, no. 2, pp. 154–161, 2016, doi: 10.1056/nejmra1601705.
- L. S. Wilson and A. J. Maeder, “Recent directions in telemedicine: Review of trends in research and practice,” *Healthc. Inform. Res.*, vol. 21, no. 4, pp. 213–222, 2015, doi: 10.4258/hir.2015.21.4.213.
- Q. Huang, Y. Chen, L. Liu, D. Tao, and X. Li, “On Combining Biclustering Mining and AdaBoost for Breast Tumor Classification,” *IEEE Trans. Knowl. Data Eng.*, vol. 32, no. 4, pp. 728–738, 2020, doi: 10.1109/TKDE.2019.2891622.
- V. Lahoura et al., “Cloud Computing-Based Framework for Breast Cancer Diagnosis Using Extreme Learning Machine,” *Diagnostics*, vol. 11, no. 2, p. 241, 2021, doi: 10.3390/diagnostics11020241.
- R. B. Trabelsi, A. D. Masmoudi, and D. S. Masmoudi, “A bi-modal palmvein palmprint biometric human identification based on fusing new CDS DP features,” *2015 Int. Conf. Adv. Biomed. Eng. ICABME 2015*, pp. 1–4, 2015, doi: 10.1109/ICABME.2015.7323236.
- A. S. Al-Waisy, R. Qahwaji, S. Ipson, S. Al-Fahdawi, and T. A. M. Nagem, “A multi-biometric iris recognition system based on a deep learning approach,” *Pattern Anal. Appl.*, vol. 21, no. 3, pp. 783–802, 2018, doi: 10.1007/s10044-017-0656-1.